Ultrasonic Wave Measurements: Frequential Energy Attenuation

Patrick GANNE, André VERVOORT, Jean-François THIMUS, Department of Civil Engineering, Université Catholique de Louvain, Louvain-la-Neuve, Belgium.

Abstract. The attenuation of ultrasonic waves (UW) in a medium is dependent of the frequency. If damage is induced in this medium, the frequency dependency of the attenuation changes. The normalised slope of the frequential attenuation (S_n) is proposed as parameter to quantify the induced damage. A first case study shows the use of S_n for in-situ UW measurements in a disturbed clay mass. In this case, the wave length (λ) << the path length (Δ). A second case study illustrates the possibilities of the use of S_n for laboratory UW measurements on limestone samples (with and without induced damage) whereby $\lambda >> \Delta$.

1. Introduction

Ultrasonic wave (UW) measurement is a common non-destructive testing method for in situ as well as for laboratory conditions. Depending on the medium, both velocity and attenuation are interesting parameters to characterise UW. The change of these parameters is interpreted as a result of a change in the internal structure of the medium.

The velocity is generally accepted as the most comprehensive parameter to study UW [14]. A variation of the velocity corresponds to a physical change of density, elastic moduli or Poisson`s coefficient of the medium [12]. Other characteristics like the pore pressure and scattering effects might have some influence too [13, 17]. Historically, UW attenuation is more difficult to obtain experimentally than UW velocities. However, recent research begins to focus more on UW attenuation measurements since UW attenuation is generally more sensitive than UW velocities for changing conditions [6]. A disadvantage is the difficult physical interpretation of the attenuation [4, 5].

The exact nature of the attenuation of UW in solids may be attributed to a number of different causes. Grain boundary losses occur as a result of the random orientation of the anisotropic grains in a polycrystalline medium. Each grain boundary represents a discontinuity of elastic modulus and, hence, in the characteristic impedance for the UW. When the wavelength (λ) is small compared to the grain size, the losses are caused by regular reflections (diffusion), which increases linearly with the frequency (ν) [9]. On the other hand, when the particle size is approximately equal to λ, the attenuation is proportional to the square of the frequency (ν^2) [9]. Finally, when λ is large compared to the grain size, Rayleigh-type scattering occurs and the attenuation is proportional to ν^4 [3]. Additional attenuation can be caused by thermal relaxation, lattice imperfections, ferromagnetic and ferroelectric properties of the medium, etc. [3, 11, 12].

UW measurements are more accurate when λ relative to the path length (Δ) is small. As a rule of thumb, when λ increases till the order of magnitudes of Δ, the variation in the velocity are barely measurable. As for the UW attenuation, this restriction is less rigorous: in most media, the variations of the UW attenuation are measurable, even when $\lambda >> \Delta$.

This paper proposes and discusses the use of the normalised slope of the frequential attenuation as an interesting parameter to analyse UW. This parameter is used on in situ UW measurements (where $\lambda << \Delta$) as well as on laboratory UW measurements (where $\lambda >> \Delta$). These two case studies shows that it is possible to use UW in the case of $\lambda << \Delta$, as well as in the case of $\lambda >> \Delta$.

2. Measuring Set-Up

2.1 In-Situ Measurements

The underground research facility HADES at Mol (Belgium) lies in the Boom clay formation at a depth of 225 m. From a main tunnel of the underground laboratory, two parallel boreholes are first drilled (diameter borehole A = 120 mm, B = 118 mm) in one sidewall. Figure 1 gives the position of these two boreholes together with borehole C. Liner tubes (diameter 108 mm) are placed in the boreholes A and B in order to prevent a total convergence of the boreholes. The liner tubes are equipped with sensors (transmitters and receivers, see table 1). After 220 days, the closure of the borehole and other phenomena are believed to become stabile. So, on day 220, borehole C (diameter of 158 mm) is drilled. The diameter of the liner tube of borehole C at the studied borehole depth is only 50 mm, which allow borehole C to converge over a distance of about 54 mm. This disturbs the clay in-situ material. Daily ultrasonic cross-hole measurements are performed (day 220 till day 487) [7].

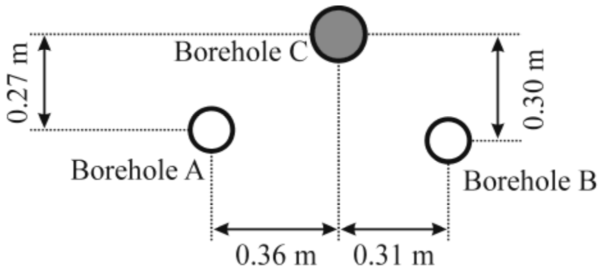

Figure 1. Configuration of the boreholes: Borehole A (diameter = 120 mm) and B (diameter = 118 mm) are drilled on day 1, borehole C (diameter = 158 mm) is drilled on day 220.

The ultrasonic waves are broad band (ν = 5 kHz to 80 kHz; λ = 20 to 320 mm) signals. They are generated and amplified to a peak-to-peak amplitude of up to 300 Volt. To get a better signal-to-noise ratio, the signals are stacked 256 times and the stacked result is stored. The sensors consist of piezoelectric elements which are embedded in a cylindrical brass housing (GMuG). The housing is mounted on a small pneumatic cylinder which mechanically presses the sensors against the borehole wall using a strong spring. The coupling elements are brass cylinder segments adapted to the borehole diameter [10].

Table 1. Overview of the locations of the transmitters and receivers, used in this study.

	Transmitter		**Receiver**	
	T3	T4	R1	R4
Borehole	B	A	B	A
Depth [m]	5.8	7.6	7.6	5.8

2.2 Laboratory Measurements

The rock material used in the laboratory tests is Belgian crinoidal limestone. This material is mainly composed of calcite, in various forms (crinoids and other bioclasts, micrite) [16]. Stylolites are frequently encountered. Test samples, containing outspoken stylolite bands are rejected for testing.

The crinoidal limestone blocks are sawed and rectified into rectangular slabs of 31 mm x 60 mm x 140 mm. At one side, half a cylinder is drilled with a diameter of 58 mm (Figure 2). The loading direction determines the stress redistribution. If the external load is applied on the short sides of the rectangular samples, compressive stresses are present adjacent to the borehole. Figure 3A shows the calculations (Flac 4.0) of the stress redistribution on the symmetrical plane when a loading force of about 80 kN (about 80% of the failure load) is applied on the short sides of a sample. This is further called the compression configuration. If the external load is applied on the long sides, both the radial and tangential stresses are negative (tensile stresses) close to the borehole. Figure 3B shows the calculated stress redistribution on the symmetrical plane when the load on the long sides of a sample rises until plastic deformation occurs (at an external load of 40 kN). This is further called the tension configuration.

The Dartec loading machine is used in the displacement-controlled mode (v = 0.001 mm/s). During the loading test, 1 mm thick Teflon is placed between the machine compression platens and the test sample, in order to minimize the frictional stresses. To quantify the damage in tension only, a load is applied on the long sides (tension configuration) until an intergranular crack of several centimetres is visualised by capillarity water [15]. This loading procedure is further referred to as T. To quantify the damage by compression only, a load is applied as in the compression configuration until 83 kN (i.e. about 80% of the peak load). This loading procedure is further referred to as C. To quantify the effects of some damage in tension, followed by damage in compression, the load is first applied as in the tension configuration (until an intergranular crack of several centimetres is visualised) before the sample is rotated by 90° (compression configuration) and loaded until 50 kN. This loading procedure is further referred to as TC.

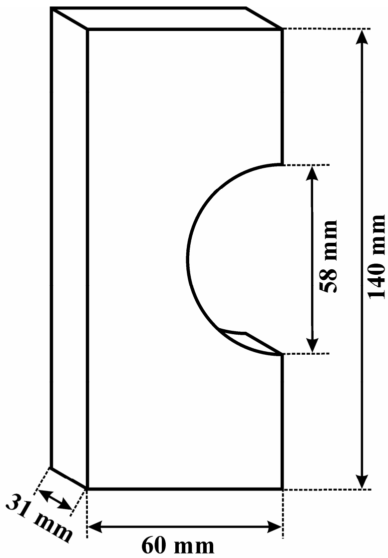

Figure 2. Geometry of the tested laboratory samples.

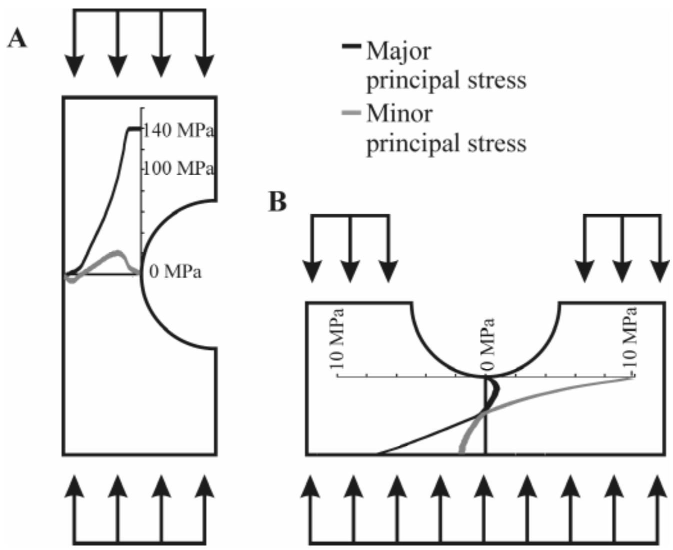

Figure 3. Presence of tensile stresses (negative) and compressive stresses (positive) in the geometry of the test samples, depending on the load direction: (A) in compression configuration and (B) in tension configuration.

The UW measurements are conducted after the samples are unloaded. In the case of C and T loadings, it means before and after the loading. In the case of the TC loading procedure, UW measurements are also conducted in between the loading in tension and in compression configuration. In order to measure UW, a PUNDIT system (CNS Electronics Ltd.) and two sensors are used in a direct transmission set-up (Figure 4A). The piezoelectric crystals converts an 800 Volt (duration = 2µs) signal into a UW (ν = 5 kHz to 90 kHz, λ = 60 mm to 1120 mm). The received signal is recorded for 200 µs and digitalised at a frequency of 5 MHz. The signals are stacked eight times, and the stacked result is stored on a computer. Afterwards, the signals are subjected to a DC filter. The transmitter (as well as the receiver) is a horn-like point sensor: they have a contact diameter of 5 mm. The horn-like transmitter permits the UW to fully develop and guides the UW into the limestone material. The point sensors enables UW measurements every 5 mm along the central line of the sample (Figure 4B).

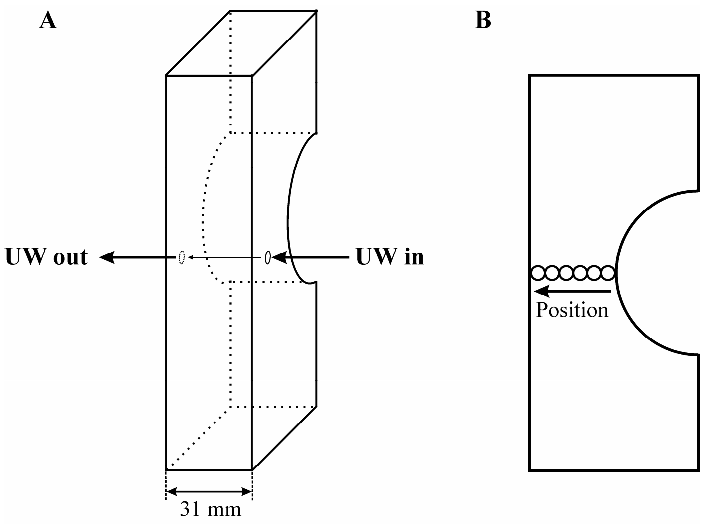

Figure 4. (A) View of the direct transmission UW, 'UW in' is the position of the transmitter and 'UW out' is the position of the receiver; (B) view of the predefined UW measurement positions (O) and the definition of the position [mm] (0 mm is at the borehole wall).

3. Frequential Energy Attenuation

The amplitude of an UW can be described as:

$$A_{out} = A_{in} e^{-\alpha(\nu)\Delta} \qquad (1)$$

where A_{in} is the amplitude of the transmitted UW, A_{out} is the amplitude of the received UW. The UW decays with a factor per unit length of travel distance through the medium. This factor is called the attenuation coefficient (α) [1/m]. Δ [m] is the path length (i.e. travel distance) of the wave in the medium [12]. When the amplitude of the transmitted UW is compared with the amplitude of the received UW, the attenuation coefficient can be calculated. As explained in the introduction, α is function of the frequency of the UW.

In function of the observed frequency range, α has a linear, parabolic or a fourth order polynomial dependency of ν [3, 11, 12]. When specific physical properties of the medium changes, the dependency of $\alpha(\nu)$ changes [1, 2]. In this study, α is supposed to be a linear function of ν [1/s]:

$$\alpha = S\nu + C \qquad (2)$$

where S represents the slope of the frequential attenuation. C is a constant which is not further discussed in this paper as it does not specify the frequency dependence of α [7]. When specific physical properties of the medium change, the slope S [s/m] changes too. S is normalised to the reference slope S_r:

$$S_n = S - S_r \tag{3}$$

S_r is calculated from a reference UW signal, which is recorded prior to damage, but using the same geometry. An increase of S_n corresponds mathematically to a relative large portion of low frequency energy in the received wave. S_n can be negative, meaning that the high frequencies are relatively less attenuated than the low frequencies.

Mathematically, S_n is calculated according to equation 4:

$$S_n = \frac{\ln\left(\dfrac{A^D_{\nu_1}}{A^D_{\nu_2}}\dfrac{A^R_{\nu_2}}{A^R_{\nu_1}}\right)}{\Delta(\nu_2 - \nu_1)} \tag{4}$$

where $A^D\nu_1$ and $A^D\nu_2$ are the amplitudes of the frequency spectrum of the received UW signal at frequency ν_1 and ν_2 respectively, and $A^R\nu_1$ and $A^R\nu_2$ are the amplitudes of the frequency spectrum of the received reference UW signal at frequency ν_1 and ν_2 respectively. It should be stressed that ν_1 and ν_2 are arbitrarily chosen, but they should stay equal during the entire experiment. The sensitivity of the result of the study is dependant on ν_1 and ν_2. It is recommended to take a ν range as large as possible into account.

4. In Situ UW Measurements (λ = 20 to 320 mm << Δ = 670 mm)

During and just after the drilling of boreholes A and B (day 1), the clay around the boreholes is disturbed and has not reached a new equilibrium. So, the physical properties of the clay around the boreholes change continuously during a period until equilibrium is reached again. Figures 5 and 6 show that S_n increases during the first 5 to 15 days after drilling, followed by a decreases during the next 60 to 80 days. Both figures indicate that S_n reaches equilibrium after about 80 to 100 days.

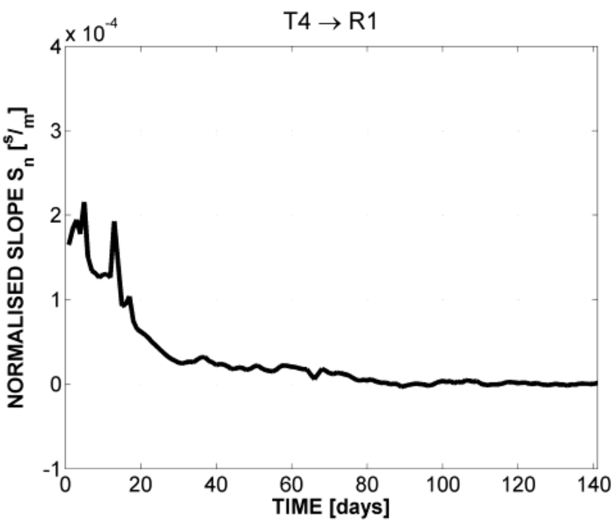

Figure 5. Variation of the normalised slope S_n [s/m] of UW measurements in clay from transmitter 4 to receiver 1, from day 1 till day 141.

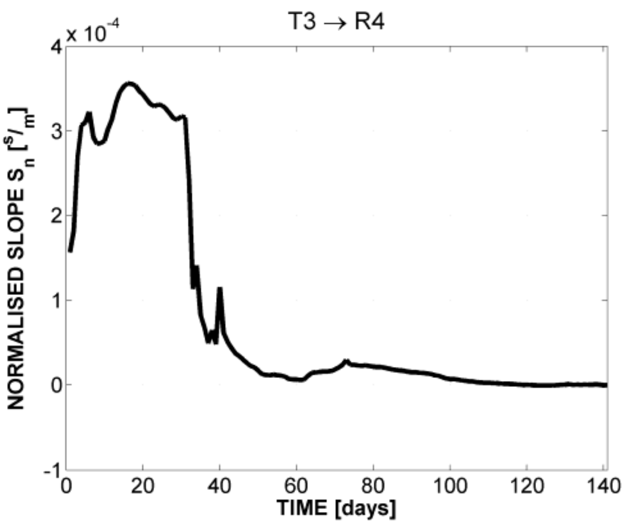

Figure 6. Variation of the normalised slope S_n [s/m] of UW measurements in clay from transmitter 3 to receiver 4, from day 1 till day 141.

At day 220, borehole C is drilled, followed by its convergence which lasts for about 100 days. This affects the properties of the surrounding clay and thus of the UW passing through the clay mass. S_n increases over the first three days, followed by a very slow decrease over the entire period of observation, being more than 250 days (Figure 7).

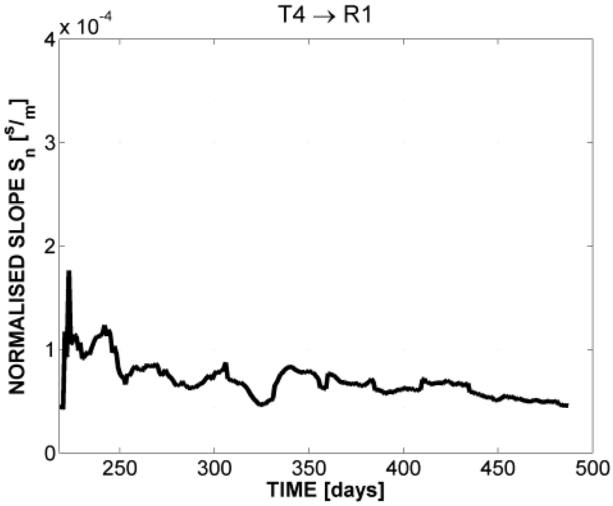

Figure 7. Variation of the normalised slope S_n [s/m] of UW measurements in clay (in situ) from transmitter 4 to receiver 1, from day 220 till 487 (drilling borehole C on day 220).

The physical interpretation of the variation of S_n is at this moment still part of further studies. It should be stressed that reaching equilibrium in the variation of S_n does not imply that the clay medium is in total equilibrium. In contrast, when S_n is still changing, one may conclude that the clay mass has not reached full equilibrium. S_n is only sensitive for specific physical properties, so when these physical properties stop altering, S_n stops varying. Although a clear physical interpretation of the variation of S_n is not given, it is clear that the clay mass evolves to an equilibrium during at least 80 days after the drilling of boreholes A and B, and at least 230 days after drilling borehole C. In the latter, the diameter of lining is about one third of the drilled diameter, while this difference in diameter A and B is 1 to 2 mm.

5. Laboratory UW measurements (λ = 60 to 1120 mm >> Δ = 31 mm)

Because Δ is very small, the variation of S_n should be measured very accurately. Therefore, it is important to have a good idea of the variation of S_n during the laboratory UW measurements. UW measurements are conducted on samples, where no damage is induced by loading. Figure 8 (samples A, B, C and D) shows four examples of variation of S_n at the predefined positions. The minimum (-6.10^{-4} s/m) and the maximum (2.10^{-4} s/m) of the variation of S_n are used as confidence limits CL, which is a very conservative methodology.

When damage is induced by a loading in the compression configuration (till 80% of the peak load), S_n decreases with the position. Figure 9 illustrates that these variations of S_n (E, F, G and H) do not exceed the confidence limits CL. When damage is induced by loading in the tension configuration (till an intergranular crack is visualised), S_n decreases with the position. Again, these variations of S_n (I, J and K) do not exceed the confidence limits CL (Figure 10). One sample (J) is additionally damaged in the compression configuration. The UW measurements which take into account the induced damaged caused by the loading in tension and in compression configuration are called J_2. Figure 11 shows that the variations of J_2 does exceed the confidence limits CL at positions 7.5 mm and 12.5 mm (i.e. close to the borehole). Thin slices of these samples are made. It has been checked under microscope that in sample J (induced damage in tension and compression configuration), far more (micro-) damage is induced than in the other samples [8]. It is also observed that most damage is induced close to the borehole. It should be stressed that the damage observed in the 0.5 mm vicinity of the borehole is likely due to the sample preparation. This could explain why the S_n (of J_2) at the 2.5 mm position does not exceed the confidence limits, while at the 7.5 mm and the 12.5 mm positions, S_n exceeds the confidence limits.

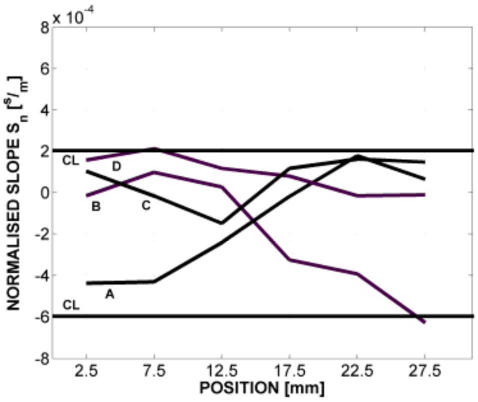

Figure 8. Overview of the variation of S_n at the predefined positions. These measurements are conducted on samples on which no damage is induced (A, B, C and D). CL indicates the confidence limits.

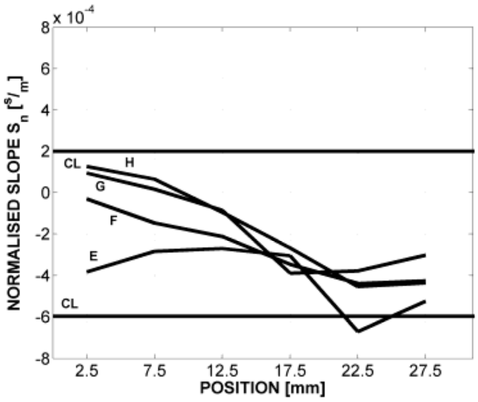

Figure 9. Overview of the variation of S_n at the predefined positions caused by damage induced by loading in compression configuration till 80 % of the peak load (E, F, G and H). CL indicates the confidence limits.

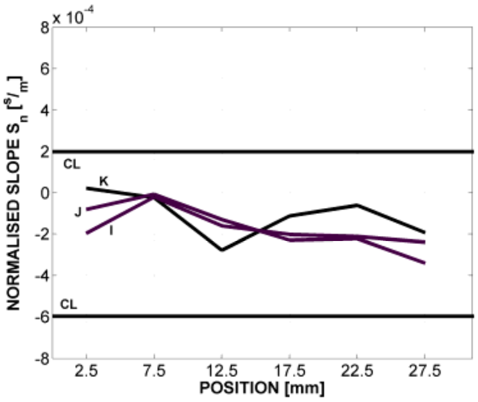

Figure 10. Overview of the variation of S_n at the predefined positions caused by damage induced by a loading in tension configuration until an intergranular crack is visualised (I, J and K). CL indicates the confidence limits.

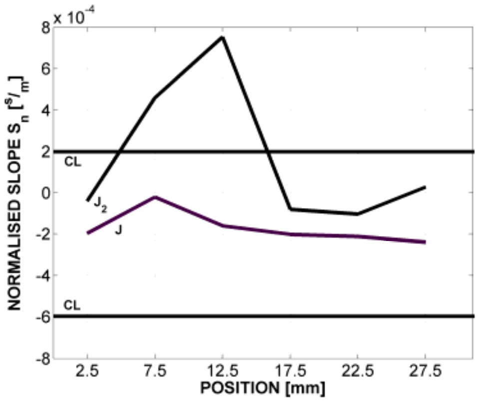

Figure 11. Overview of the evolution of S_n at the predefined positions. J indicates S_n when only damage is induced caused by a loading in tension configuration until an intergranular crack is visualised (see Figure 10); J_2 indicates S_n when a successive loading in compression configuration (until 50 kN) induced additional damage. CL indicates the confidence limits

A straightforward physical interpretation of the variation of S_n can still not be given. But it is clear that when enough additional (micro-) damage is induced, S_n does alter beyond the confidence limits CL (Figure 11). Similar UW measurements confirm this observation. It should be stressed that in these measurements (i.e. $\lambda >> \Delta$), the waves are influenced by the geometry of the samples. This influence is taken into account if the UW measurement is compared to a reference UW signal (as in equation 3 and 4). In this reasoning, it is important that the reference UW signal is measured on the same sample prior to damage but using the same geometry.

6. Conclusions

The normalised slope (S_n) of the (linear) frequency dependency of the attenuation (α) is proposed as a typical parameter to characterise ultrasonic waves (UW). S_n is function of the 'damage' in the medium. A daily UW measurement in disturbed clay mass is used to illustrate the actual possibilities of S_n. These in-situ UW measurements preserve the typical case that the wave length (λ) << the path length (Δ). The possibilities of S_n are further studied on UW measurements on small crinoidal limestone samples. In these laboratory conditions, $\lambda >> \Delta$. If enough (micro-) damage is induced in the limestone, the parameter S_n is sufficiently sensitive to characterise the damage even though $\lambda >> \Delta$. Further research is necessary in order to quantify the influence of (micro-) cracks, fractures, pore pressure, E-modulus, Poisson`s coefficient, etc.

Acknowledgements

The financial support of the Research Council of the Katholieke Universiteit Leuven (OT-project) is gratefully appreciated.

References

[1] Bartleson V.B., Viggen K., Asanuma T., Kinnick R.R. and Belohlavek M., 2003. Automated quatitative analysis of the shift of frequency spectra generated by attenuated signals from contrast microbubbles. Ultras. 41, 75-81.
[2] Biwa S., Watanabe Y., Motogi S. and Ohno H., 2004. Analysis of ultrasonic attenuation in particle-reinforced plastic by a differential scheme. Ultras. 42, 5-12.
[3] Blitz J., 1967. Fundamentals of ultrasonics. Butterworths, London, 220p.
[4] Couvreur J.F., 1997. Propagation d'ondes ultrasoniques dans des roches sédimentaires, étude de l'endommagement par traitement des signaux. UCL, Louvain-la-Neuve, 220p.
[5] Diallo M.S., Prasad M. and Appel E., 2003. Comparison between experimental results and theoretical predictions for P-wave velocity and attenuation at ultrasonic frequency. Wave Motion 37, 1-16.
[6] Donald J.A., Butt S.D. and Iakovlev S., 2004. Adaptation of a triaxial cell for ultrasonic P-wave attenuation, velocity and acoustic emission measurements. Int. J. Rock Mech. Min. Sci. 41, 1001-1011.
[7] Ganne P., Vervoort A. and Bastiaens W., 2006. In situ ultrasonic wave measurements in clay: comparison between velocity, frequential attenuation and energy. Eurock 06, Multiphysics coupling and long term behaviour in rock mechanics. Liège.
[8] Ganne P. and Vervoort A., 2006. Characterisation of tensile damage in rock samples induced by different stress paths. Pure and Apll. Geophys., 163, in press.
[9] Gaydecki P.A., Burdekin F.M., Damaj W., John D.G. and Payne P.A., 1992. The propagation and attenuation of medium-frequency ultrasonic waves in concrete: a signal analytical approach. Maes. Sci. Technol. 3, 126-134.
[10] Manthei G., 2005. Long-term seismic and acoustic emission measurements estimating the evolution of the excavation disturbed zone with time. GMuG report.
[11] Mason P.W., 1958. Physical acoustics and the properties of solids. Van Nostrand, Princeton, 402p.
[12] Mason P.W., 1968. Physical acoustics, Principles and Methods. Academic Press, New York, 490p.
[13] Philippidis T.D. and Aggelis D.G., 2005. Experimental study of wave dispersion and attenuation in concrete. Ultras. 43, 584-595.
[14] Ragozzino M., 1981. Analysis of the error in measurement of ultrasound speed in tissue due to waveform deformation by frequency-dependent attenuation. Ultras. 19, 135-158.
[15] Van de Steen B., 2001. Effect of heterogeneity and defects on the fracture pattern in brittle rock. PhD thesis, KULeuven, Leuven, 249p.
[16] Van de Steen B., Vervoort A. and Sahin K., 2002. Influence of internal structure of crinoidal limestone on fracture paths. Eng. Geol. 67, 109-125.
[17] Zhao B., Basir O.A. and Mittal G.S., 2005. Estimation of ultrasound attenuation and dispersion using short time Fourier transform. Ultras. 43, 375-381.